IET Microwaves, Antennas & Propagation

Research Article

IET Journals
The Institution of Engineering and Technology

Impedance matching bandpass filter with a controllable spurious frequency based on λ/2 stepped impedance resonator

ISSN 1751-8725
Received on 4th April 2018
Accepted on 10th May 2018
E-First on 12th July 2018
doi: 10.1049/iet-map.2018.5127
www.ietdl.org

Phirun Kim[1], Girdhari Chaudhary[1], Yongchae Jeong[1] ✉

[1]*Division of Electronics and Information Engineering, IT Convergence Research Center, Chonbuk National University, Jeollabuk-do, Jeonju 561-756, Republic of Korea*

✉ *E-mail: ycjeong@jbnu.ac.kr*

Abstract: An impedance matching bandpass filter (BPF) with arbitrary image impedance (Z_2) of parallel/antiparallel coupled lines SIR is presented in this study. The proposed structures consist of conventional SIRs and additional transmission lines with an electrical length of $\pi/2-\theta_2$ at the input and output ports. Moreover, the coupling coefficients of the coupled line can be controlled by the image impedance and it does not affect the bandpass responses. Since the first spurious frequency of the conventional SIR BPF can be suppressed with a transmission zero by using antiparallel coupled lines, the proposed BPF can provide wide stopband and high attenuation characteristics. For the experimental validation of the proposed filter, three types of BPFs with 20–50 and 50–100 Ω termination impedances were designed and fabricated at the operating centre frequency (f_0) of 2.6 GHz. By using the antiparallel coupled line instead of the parallel coupled line, the first spurious frequency is occurred at $3.71f_0$ and the stopband rejection considerably improved.

1 Introduction

The impedance matching bandpass filter (BPF) with a wide stopband characteristic plays an important role in modern microwave communication systems of suppressing unwanted signals and miniaturised size. Fig. 1*a* shows the conventional RF front-end receiver of communication systems [1]. In addition to the frequency selective and wide stopband characteristics, the impedance matching BPF can directly match the input and output impedances of the transistor or input impedance of the antenna to reduce the circuit size, cost, non-negligible insertion loss, and the complexity of the network as can be seen in Fig. 1*b*. Therefore, unequal termination impedance BPF with controllable spurious frequencies is a new design challenge for modern communication systems [2].

General BPFs have typically been analysed and designed with equal termination impedances (50–50 Ω) [3–8]. In [3], the generally designed formulas of parallel coupled line BPF were derived for Chebyshev and Butterworth responses assuming termination impedances (Z_0) equalled to the image impedance of the coupled lines. Meanwhile, the modified design methods of equal termination impedance parallel coupled line BPF with an arbitrary image impedance were introduced in [4–6]; however, they were valid only for the parallel-coupled half-wavelength resonator and their spurious frequencies were typically produced at $2f_0$ and $3f_0$. Moreover, the alternative J/K inverter BPF was designed with wide stopband characteristics [7]. However, the design equations were applicable for even-order Chebyshev response and equal termination impedance. In [8], a half-wavelength parallel/antiparallel coupled line BPF with arbitrary coupling lengths of the coupled line was presented for second and third harmonics suppression by the transmission zeros. This filter is only valid for termination impedance equalled to the image impedance of the coupled line.

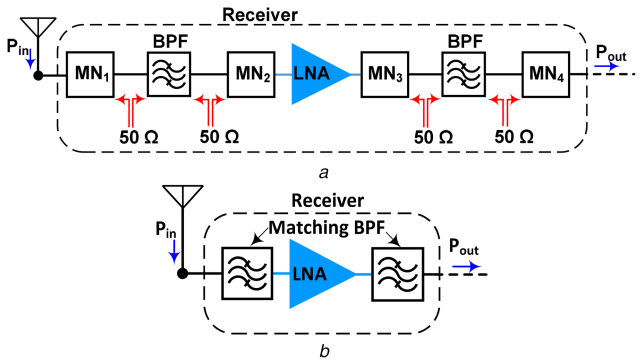

Fig. 1 *RF front-end receiver of communication system with*
(a) Conventional matching networks and filters and ***(b)*** Using matching BPFs

Recently, impedance matching networks with a bandpass response were analysed [9–18]. In [9–11], narrow band high-Q cavity BPFs with one, two, and three poles were analysed using a coupling matrix to directly match the output impedance of the transistor. However, the design equations were not applicable for microstrip lines BPFs. For microstrip technology, the ladder networks of unequal termination impedances low-pass filters [12, 13] were used to design the input and output matching networks [14–16] of the transistor using the optimising technique. However, the lower-side stopband (closed to DC) characteristic of [13] was poor and varied with termination impedance ratio ($r = R_S/R_L$). In [17], unequal termination impedance parallel-coupled half-wavelength resonator BPF was presented using an optimisation process with a low r. Subsequently, a new analysis of unequal termination impedance parallel-coupled microstrip half-wavelength resonator BPF was introduced in [18] with a higher r and arbitrary image impedance of the coupled line. However, the spurious frequency is poor. In [19–21], a coupled line impedance transformer with a shunt TL and its applications in the power divider and power amplifier were presented. In these works, a half-wavelength ($\lambda/2$) shunt open-stub TL was used to produce transmission zero at $0.5f_0$, $1.5f_0$, and $2.5f_0$ and to enhance the r. However, the sharp roll-off characteristic was limited with the one-stage coupled line. In [22], the impedance transformer was analysed using a two-stage coupled line to obtain better frequency selectivity and higher r compared to those in [19]. However, stopband attenuation, the bandwidth of the passband, and a number of stages cannot be specified and the $2f_0$ and $3f_0$ were not suppressed. In [23], the bandwidth of the passband can be enhanced using the two-stage coupled line, but the r is still low.

A non-uniform resonator known as a stepped impedance resonator (SIR) was introduced in [24] and was widely used to

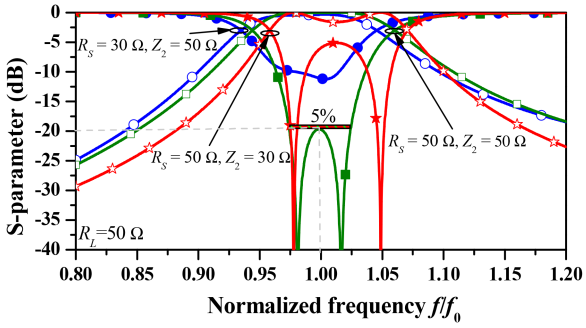

Fig. 2 *Conventional SIR BPF [25] with different termination impedance and image impedance of the coupled line*

control spurious frequencies for wide stopband characteristics. In [25, 26], parallel coupled line SIR BPFs were synthesised with various stepped impedance ratios (K). However, these conventional SIR BPFs also require image impedance of a coupled line equalled to the termination impedance (i.e. $Z_2 = Z_0$) to avoid mismatching. The analyses of unequal termination impedance BPF of [27–30] were not applicable for all kinds of resonators especially microstrip coupled line SIR BPFs. Fig. 2 shows the S-parameters of the conventional SIR BPF with different termination impedances and Z_2. The filters are mismatched and frequency-shifted when termination impedances and Z_2 are not the same. Therefore, additional networks or new analyses are required to solve these issues.

In this paper, new general design formulas of impedance matching BPF with an arbitrary image impedance of $\lambda/2$ parallel/antiparallel coupled line SIR are analysed and implemented on a microstrip line. By simply adding TLs to the input and output ports of SIR BPF with a specific length and characteristic impedances, the image impedance of parallel/antiparallel coupled lines and termination impedances can be selected arbitrarily. In addition, the arbitrary termination impedance of the proposed BPF can suppress the first spurious frequency of the conventional SIR BPF with a transmission zero and provide a high spurious and high attenuation performance.

2 Circuit analysis

2.1 Equivalent circuit

Fig. 3*a* shows a basic configuration of a conventional half-wavelength parallel coupled line SIR BPF. Similarly, Figs. 3*b* and *c* show the schematics of the proposed impedance matching SIR BPF using parallel and antiparallel coupled lines, respectively. The proposed structure I consists of conventional SIRs and additional TLs with characteristic impedance of Z_2 and electrical length of $\pi/2-\theta_2$ at the input and output ports. In the proposed structure II, the intermediate parallel coupled lines of the proposed structure I are replaced with antiparallel coupled lines. Fig. 4*a* shows the equivalent circuit of Fig. 3*a* [25]. Since the electrical length of θ_2 is less than $\lambda/4$, the input and output admittances Y_{1S} and Y_{1L} would be complex admittance under the condition of $Y_0 \neq Y_2$. Therefore, the image impedance of the coupled line in the conventional SIR filters must be the same as termination impedance (typically 50 Ω) to avoid mismatching. Thus, it has a tight limitation to design a wide stopband characteristic BPF due to realisation difficulty in microstrip line. Fig. 4*b* shows the equivalent circuit of the proposed SIR BPFs shown in Figs. 3*b* and *c*. The additional TLs plays an important role in the proposed circuit. The electrical length of the coupled line and additional TL at the input and output ports is $\pi/2$ at f_0; therefore, Y_{1S} and Y_{1L} are always the real admittances, then image admittance of coupled line can be chosen arbitrarily. Finally, the adjacent J-inverter at the input and output ports can be matched with a specific bandwidth and termination impedances. Thus, the proposed filters can be designed as impedance matching SIR BPFs. From Fig. 4*b*, the input admittance Y_{1S} looking into the source from $J_{0,1}$ is obtained as follows:

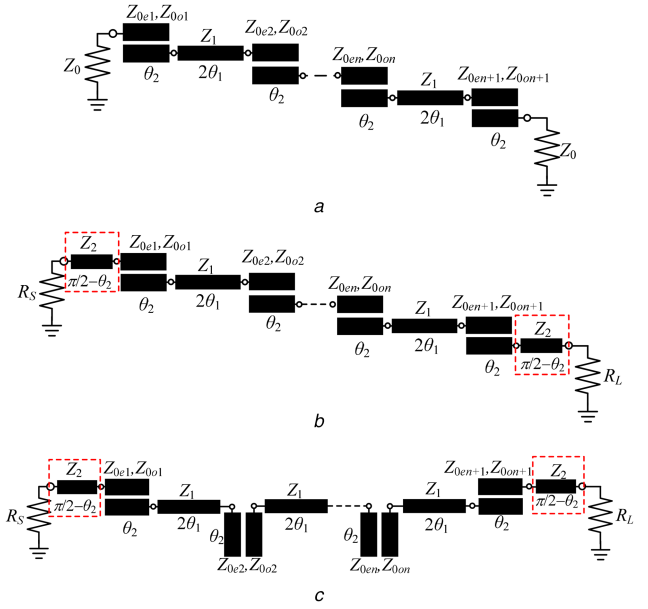

Fig. 3 *Paralle coupled line BPFs with stepped impedance resonators*
(a) Conventional [25], ***(b)*** Proposed structure I of impedance matching BPF with parallel coupled lines, and ***(c)*** Proposed structure II of impedance matching BPF with antiparallel coupled lines

$$Y_{1S} = \frac{Y_2^2}{G_S}, \tag{1}$$

where Y_2 ($Y_2 = 1/Z_2$) is an image admittance of the coupled line. Similarly, the output admittance of Y_{1L} looking into the load from $J_{n,n+1}$ is obtained as follows:

$$Y_{1L} = \frac{Y_2^2}{G_L}, \tag{2}$$

where $G_S = 1/R_S$ and $G_L = 1/R_L$ are the termination source and load conductances, respectively.

2.2 Stepped impedance resonator and J-inverter

In the case of $\theta_1 = \theta_2 = \theta_0$, the resonant frequencies can be found as [28]

$$\theta_0(f_0) = \tan^{-1}\sqrt{K}, \tag{3}$$

where

$$K = \frac{Y_1}{Y_2} = \frac{Z_2}{Z_1}, \tag{4}$$

and K is a ratio of two characteristic admittances of SIR.

Fig. 5 shows the variations of characteristic impedance Z_1 and the total electrical length ($\theta_T = 4\theta_0$) of the SIR according to K and Z_2. The total length of the resonator is longer than $\lambda/2$ with $K > 1$ and less than $\lambda/2$ with $K < 1$. For the same K, the characteristic impedance Z_1 is increased as Z_2 increases. The Z_2 can be chosen arbitrarily after adding TLs to the input and output of conventional SIR filters. Thus, the filter can be realised with a low K when compared to the conventional SIR BPF.

The general J-inverters of arbitrary termination and arbitrary image admittance of parallel/antiparallel coupled line SIR BPF are given as follows:

$$J_{0,1} = Y_2\sqrt{\frac{2\theta_0 Y_2 FBW}{G_S g_0 g_1}}, \tag{5a}$$

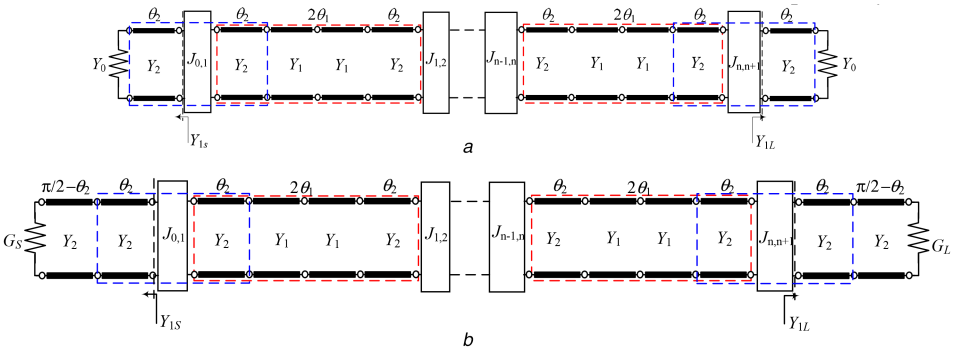

Fig. 4 *Equivalent circuits of parallel coupled line stepped impedance resonators*
(a) Conventional circuit and ***(b)*** Proposed circuits I and II

$$J_{i,i+1} = 2\theta_0 Y_2 \mathrm{FBW}\sqrt{\frac{1}{g_i g_{i+1}}}, \quad i = 1, 2, \ldots, n-1 \tag{5b}$$

$$J_{n,n+1} = Y_2\sqrt{\frac{2\theta_0 Y_2 \mathrm{FBW}}{G_L g_n g_{n+1}}}, \tag{5c}$$

where g_0, g_1, …, and g_{n+1} are the prototype low-pass element values, which can be computed for either Chebyshev (or equal-ripple) or Butterworth (or maximally flat) responses [27], and FBW is a fractional bandwidth of the passband. In the case of $Y_2 = G_S = G_L = Y_0$, the J-inverters of (5) are the same as those of the conventional SIR BPF. The design formulas of multi-stage impedance matching SIR BPF with arbitrary image impedances of coupled lines can be directly adopted to design a practical filter.

The relative formulas between the coupled line and the J-inverter can be derived from the ABCD matrix. More generally, the even- and odd-mode impedances (Z_{0e} and Z_{0o}) of each parallel coupled line are derived as follows:

$$(Z_{0e})_{i+1}|_{i=0 \text{ to } n} = Z_2\frac{1 + J_{i,i+1}Z_2\csc\theta_0 + J_{i,i+1}^2 Z_2^2}{1 - J_{i,i+1}^2 Z_2^2\cot^2\theta_0}, \tag{6a}$$

$$(Z_{0o})_{i+1}|_{i=0 \text{ to } n} = Z_2\frac{1 - J_{i,i+1}Z_2\csc\theta_0 + J_{i,i+1}^2 Z_2^2}{1 - J_{i,i+1}^2 Z_2^2\cot^2\theta_0}. \tag{6b}$$

Similarly, the antiparallel coupled line has been studied and used in many applications [8, 31, 32]. In contrast to the parallel coupled line, the antiparallel coupled line of $\lambda/2$ SIR provides a transmission zero at the first spurious frequency for all K. Since the antiparallel coupled line can be used for $\theta_0 \neq \pi/2$ at f_0, it can be applied in SIR BPF with θ_0 of the coupled lines are always less than $\pi/2$. The Z_{0e} and Z_{0o} of each antiparallel coupled line are derived as follows:

$$(Z_{0e})_{i+1}|_{i=0 \text{ to } n} = Z_2\frac{1 + J_{i,i+1}Z_2\csc\theta_0\sec\theta_0 + J_{i,i+1}^2 Z_2^2}{1 - J_{i,i+1}^2 Z_2^2\cot^2\theta_0}, \tag{7a}$$

$$(Z_{0o})_{i+1}|_{i=0 \text{to} n} = Z_2\frac{1 - J_{i,i+1}Z_2\csc\theta_0\sec\theta_0 + J_{i,i+1}^2 Z_2^2}{1 - J_{i,i+1}^2 Z_2^2\cot^2\theta_0}. \tag{7b}$$

Since the antiparallel coupled line requires stronger coupling coefficients than the parallel coupled line, the intermediate coupled lines, except the first and last coupled lines, are designed with an antiparallel coupled line in the proposed network II.

3 Design examples

The design procedures of proposed impedance matching BPF are summarised with the design flowchart as shown in Fig. 6. To demonstrate the analysis, the lossless transmission lines (TLs) were used to simulate the proposed impedance matching BPFs with arbitrary Z_2. The design examples are calculated with $n = 2$, 3, 4 and FBW of 5% for the Chebyshev response (ripple = 0.0434 dB).

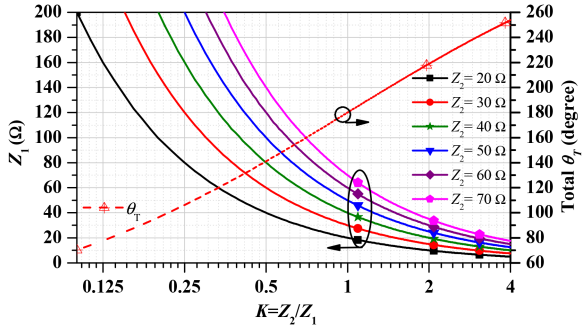

Fig. 5 *Variations of Z_1 and total electrical length of stepped impedance resonator according to K of SIR and Z_2*

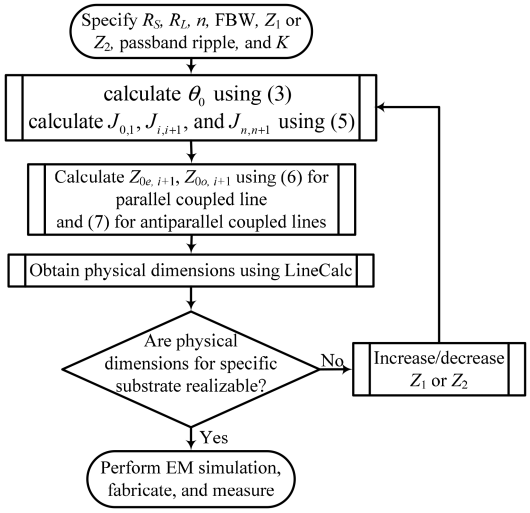

Fig. 6 *Design flowchart of proposed impedance matching BPF*

3.1 Parallel coupled line SIR BPF

Fig. 7*a* shows the S_{21} characteristics with different n. As shown in the figure, the stopband rejection becomes steeper as n increases. Also, the first spurious frequency is located at $2.25f_0$ with $K = 0.7$. Similarly, Fig. 7*b* shows the S_{21} characteristics with different K. As observed from these results, the spurious frequencies are significantly shifted from the passband of $1.77f_0$ to $2.8f_0$ with K varying from 1.5 to 0.4. The passband bandwidth is still maintained, although the spurious frequency has shifted and termination impedances are not the same. Fig. 7*c* shows the S_{21} characteristics with different Z_2 by fixing $K = 0.7$ and $n = 4$. The passband characteristic is maintained for different Z_2. However, lower- and upper-side stopband rejection characteristics are improved with high Z_2. Thus, high Z_2 is preferable for the high stopband rejection characteristic. From this simulation, it has proved the coupled line image impedance of proposed impedance matching BPF can be chosen arbitrarily. Fig. 7*d* shows the S_{21}

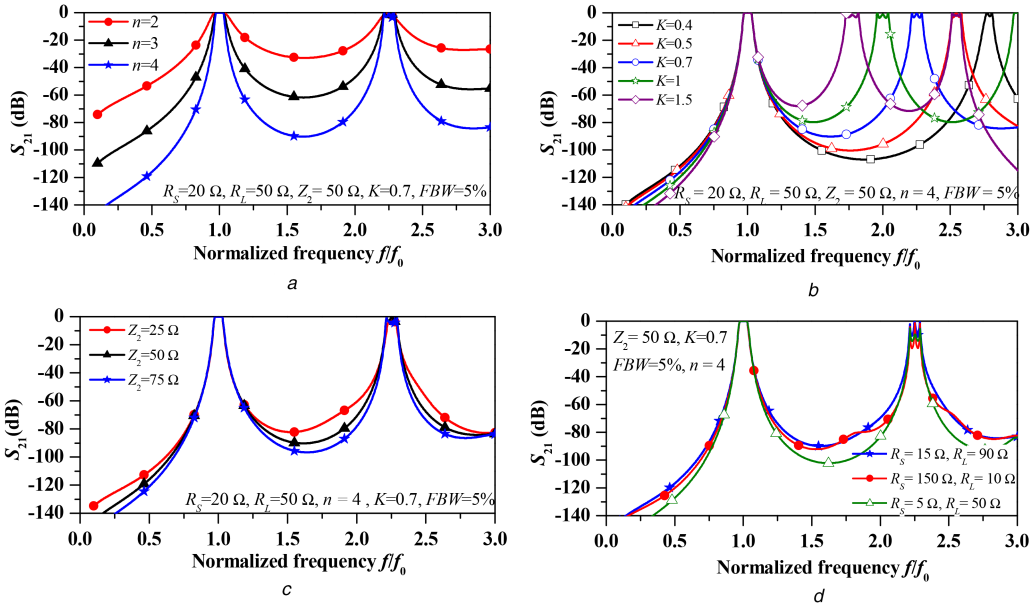

Fig. 7 *S_{21} characteristics of parallel coupled line impedance matching SIR BPF using Chebyshev response with different* ***(a)*** *n,* ***(b)*** *K,* ***(c)*** *Z_2,* and ***(d)*** Termination impedance

Table 1 Calculated values of impedance matching parallel coupled line SIR BPF using Chebyshev response with different *n*, *k*, Z_2, and termination impedance

$f/f_0 = 1$, FBW = 5%, $L_{Ar} = 0.0434$dB						
Z_{0e}/Z_{0o}, Ω	$R_S = 20\,\Omega$, $R_L = 50\,\Omega$, $Z_2 = 50\Omega$, $K = 0.7$					*n*
72.34/38.45	63.62/39.69	94.52/35.31				2
68.93/39.39	57.98/43.28	57.98/43.28	86.42/36.02			3
67.85/39.72	56.97/44.01	55.26/45.32	56.97/44.01	83.98/36.31		4
		$R_S = 20\,\Omega$, $R_L = 50\,\Omega$, $n = 4$			*K*	θ_0, deg.
69.98/39.02	56.18/44.74	54.66/45.89	56.18/44.74	89.54/35.37	0.4	32.3
69.03/39.33	56.46/44.49	54.86/45.69	56.46/44.49	87.01/35.77	0.5	35.3
67.85/39.72	56.97/44.01	55.26/45.32	56.97/44.01	83.98/36.31	0.7	39.9
66.91/40.06	57.7/43.32	55.82/44.79	57.7/43.32	81.59/36.79	1	45
66.15/40.34	58.81/42.27	56.67/43.97	58.81/42.27	79.68/37.21	1.5	50.8
		$R_S = 20\,\Omega$, $R_L = 50\,\Omega$, $n = 4$				Z_2, Ω
39.37/18.55	28.49/22	27.63/22.66	28.49/22	55.66/17.38		25
67.85/39.72	56.97/44.01	55.26/45.32	56.97/44.01	83.98/36.31		50
95.7/61.76	85.46/66.01	82.89/67.98	85.46/66.01	112.83/56.69		75
		$n = 4$, $Z_2 = 50\Omega$				R_S/R_L, Ω
144.21/35.77	56.46/44.49	54.86/45.69	56.46/44.49	61.58/42.12		150/10
57.72/44.11	56.97/44.01	55.26/45.32	56.97/44.01	83.98/36.31		5/50
64.85/40.76	56.46/44.49	54.86/45.69	56.46/44.49	105.54/34.84		15/90

characteristics with different termination impedances. The termination impedance can be terminated with a low and/or high impedance. The stopband attenuation is more attenuated with a low termination impedance. However, the passband characteristics are almost the same. Thus, the changing termination impedance does not seriously affect the operating band characteristics. It can be observed herein that the proposed impedance matching SIR BPF can be designed with arbitrary termination impedance after adding TLs at the input and output ports. The specifications and calculated circuit parameters for the simulation in Fig. 7 are shown in Table 1. The higher or lower *r* can prevent the realisation of the first and last coupled lines. This issue can be solved by decreasing or increasing the Z_2 values, which already explained in the design flowchart. However, the realisation is still limited for a very high/low Z_2 values.

3.2 Antiparallel coupled line SIR BPF

Fig. 8*a* shows the S_{21} characteristics of the proposed impedance matching SIR BPF with antiparallel coupled line and different *n*. As seen in the figure, the stopband rejection characteristics become steeper as *n* increases. Also, the first spurious frequency of design example 3.1 is suppressed significantly with the transmission zero and provides wider stopband characteristic.

Fig. 8*b* shows the S_{21} characteristics with different Z_2. In this case, the passband characteristics are maintained with different Z_2. While the stopband rejection is improved with higher Z_2, it can render Z_1 difficult to realise. Fig. 8*c* shows the S_{21} characteristics with different *K*. The first spurious frequencies are shifted from $2.4f_0$ to $4.6f_0$ as *K* decreases from 1.5 to 0.4. Thus, the proposed antiparallel coupled line impedance matching SIR BPF not only can shift the first spurious to higher frequency but also more attenuate the stopband performance compared to the parallel coupled line impedance matching SIR BPF. Similarly, Fig. 8*d* shows the S_{21} characteristics with different termination impedances. As *r* becomes higher, the stopband characteristic is improved. However, the stopband rejections near the passband are almost similar. Therefore, the antiparallel coupled line impedance matching SIR BPF provides wider stopband and steeper

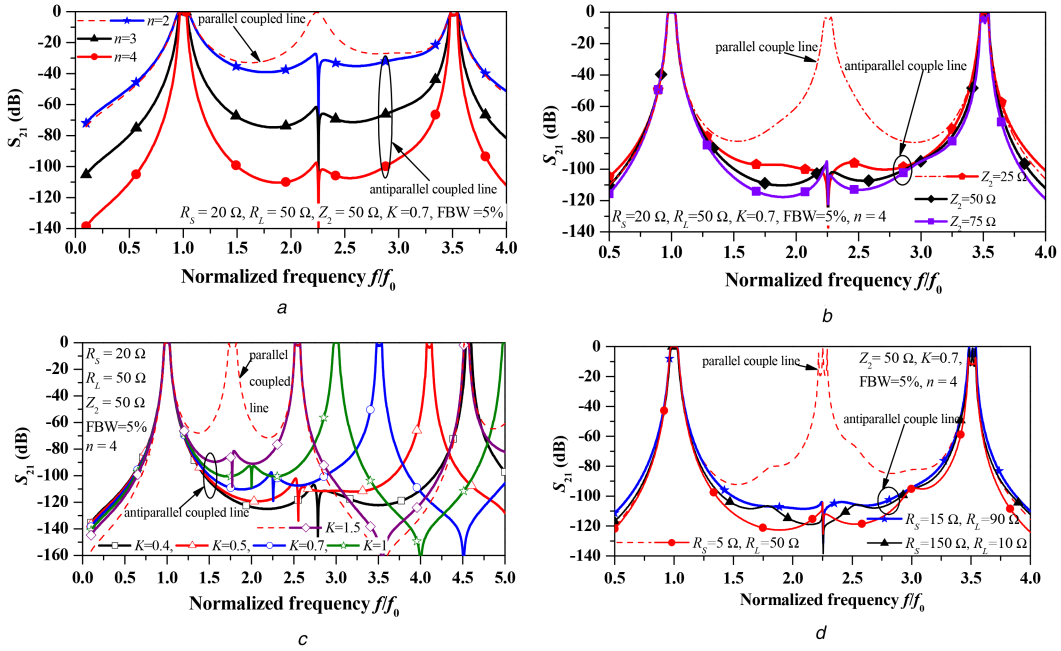

Fig. 8 *S_{21} characteristics of antiparallel coupled line impedance matching SIR BPF using Chebyshev response with different* ***(a)*** *n,* ***(b)*** *Z_2,* ***(c)*** Different K_2, and ***(d)*** Termination impedances

Table 2 Calculated values of impedance matching antiparallel coupled line SIR BPF using Chebyshev response with different *n*, *k*, Z_2, and termination impedances

$f/f_0 = 1$, FBW = 5%, $L_{Ar} = 0.0434$dB							
Z_{0e}/Z_{0o}, Ω	$R_S = 20\,\Omega$, $R_L = 50\,\Omega$, $Z_2 = 50\,\Omega$, $K = 0.7$						*n*
	72.34/38.45	60.83/42.47	94.52/35.31				2
	68.93/39.39	56.26/44.99	56.26/44.99	86.42/36.02			3
	67.85/39.72	55.46/45.52	54.1/46.48	55.46/45.52	83.98/36.31		4
	$R_S = 20\,\Omega$, $R_L = 50\,\Omega$, $n = 4$					*K*	θ_0, deg.
	69.98/39.02	55.29/45.63	53.98/46.57	55.29/45.63	89.54/35.37	0.4	32.3
	69.03/39.33	55.36/45.59	54.02/46.53	55.36/45.59	87.01/35.77	0.5	35.3
	67.85/39.72	55.46/45.52	54.1/46.47	55.46/45.52	83.98/36.31	0.7	39.9
	66.91/40.06	55.59/45.43	54.2/46.4	55.59/45.43	81.59/36.79	1	45
	66.15/40.34	55.77/45.31	54.33/46.31	55.77/45.31	79.68/37.21	1.5	50.8
	$R_S = 20\,\Omega$, $R_L = 50\,\Omega$, $n = 4$						Z_2, Ω
	39.37/18.55	27.73/22.76	27.05/23.24	27.73/22.79	55.66/17.38		25
	67.85/39.72	55.46/45.52	54.1/46.48	55.46/45.52	83.98/36.31		50
	95.7/61.76	83.19/68.28	81.15/69.71	83.19/68.28	112.83/56.69		75
	$n = 4$, $Z_2 = 50\Omega$						R_S/R_L, Ω
	144.21/35.77	55.46/45.52	54.1/46.48	55.46/45.52	61.58/42.12		150/10
	57.72/44.11	55.46/45.52	54.1/46.48	55.46/45.52	83.98/36.31		5/50
	64.85/40.76	55.46/45.52	54.1/46.47	55.46/45.52	105.54/34.84		15/90

characteristics than the parallel coupled line impedance matching SIR BPF. The specification and calculated circuit parameters for the simulations shown in Fig. 8 are listed in Table 2. From the above simulation results, it has proved that the proposed impedance matching SIR BPFs can be designed not only with unequal termination impedances but also arbitrary image impedance of coupled line after adding TLs at the input and output ports. Moreover, in practical design it is desirable to choose an antiparallel coupled line impedance matching SIR BPF with a low *K* if wide stopband and high attenuation characteristics are desired.

4 Simulation and measurement results

For demonstration, three impedances matching SIR BPFs with arbitrary terminations and Z_2 were designed and implemented on a single substrate of RT/Duriod 5880 with a dielectric constant (ε_r) of 2.2 and thickness (h) of 0.787 mm. Three types of BPFs were designed at $f_0 = 2.6$ GHz. The specifications and calculated circuit parameters are shown in Table 3. Figs. 9*a–c* show the layouts of the fabricated impedance matching SIR BPFs of two-stage parallel coupled line, two-stage antiparallel coupled line, and three-stage parallel coupled line, respectively. The physical dimensions of propose circuits are shown in Table 4.

4.1 Two-stage SIR BPF

The first BPF was designed with Chebyshev response for the following specifications: ripple = 0.043 dB, $R_S = 20\,\Omega$, $R_L = 50\,\Omega$, $Z_2 = 60\,\Omega$, $K = 0.5$, $n = 2$, and FBW = 5%. The fabricated circuit looks similar to the conventional SIR BPF, but the characteristics impedance at the input/output TLs of proposed circuit are different to the conventional one. The input/output TLs of conventional SIR BPF are fixing to be Z_0 for the measurement purpose. However, the input/output TLs of proposed SIR BPF have a characteristic impedance of Z_2, which can be chosen arbitrarily. Moreover, the electrical length of the input and output TLs can be calculated

Table 3 Calculated values of the proposed BPFs

$f_0 = 2.6$ GHz, FBW = 5%, $L_{Ar} = 0.0434$ dB						
Z_{0e}/Z_{0o}, Ω	$R_S = 20\,\Omega$, $R_L = 50\,\Omega$, $Z_2 = 60$, $K = 0.5$, $n = 2$				θ_0, deg.	first and third filters
	85.33/46.48	72.75/51.08 75.18/48.65 (shunt coupled line)		110.43/42.3	35.26	
	$R_S = 50\,\Omega$, $R_L = 100\,\Omega$, $Z_2 = 90$, $K = 1.5$, $n = 3$				θ_0, deg.	second filter
	128.64/69.78	101.78/80.67	101.78/80.67	152.83/65.73	48.75	

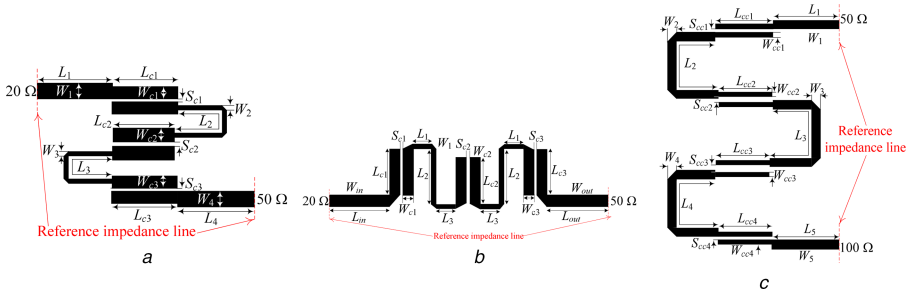

Fig. 9 *Layout of impedance matching SIR BPF using Chebyshev response*
(a) Two-stage parallel coupled lines, ***(b)*** Two-stage antiparallel coupled lines, and ***(c)*** Three-stage parallel coupled lines

Table 4 Physical dimensions of fabricated two-stage and three-stage impedance matching parallel/antiparallel coupled lines SIR BPFs using Chebyshev response (unit: mm)

Two-stage parallel coupled lines				
$W_1 = W_4 = 1.8$	$W_{c1} = 1.36$	$W_{c2} = 1.65$	$W_{c3} = 1$	$W_2 = W_3 = 0.4$
$L_1 = L_4 = 12.8$	$S_{c1} = 0.23$	$S_{c2} = 0.5$	$S_{c3} = 0.102$	$L_2 = L_3 = 17.1$
$L_{c1} = 8.49$	$L_{c2} = 8.05$	$L_{c3} = 8.6$		

Two-stage antiparallel coupled lines				
$W_{in} = W_{out} = 1.8$	$W_{c1} = 1.36$	$W_1 = 0.42$	$S_{c2} = 0.37$	$S_{c3} = 0.11$
$L_{in} = L_{out} = 12.8$	$S_{c1} = 0.23$	$L_2 = 10.5$	$L_{c2} = 8$	$L_{c3} = 8.6$
$L_{c1} = 8.49$	$L_1 = L_3 = 3$	$W_{c2} = 1.85$	$W_{c3} = 1$	

Three-stage parallel coupled lines					
$W_1 = W_5 = 0.9$	$W_{cc1} = 0.5$	$L_{cc2} = 11.2$	$L_{cc3} = 11.28$	$W_{cc3} = 0.59$	$S_{cc4} = 0.27$
$L_1 = L_5 = 9.95$	$S_{cc1} = 0.5$	$S_{cc2} = 1.47$	$S_{cc3} = 1.45$	$L_{cc4} = 11.4$	$W_{cc4} = 0.55$
$L_{cc1} = 11.2$	$W_{cc2} = 0.8$	$W_2 = W_3 = W_4 = 1.45$		$L_2 = L_3 = L_4 = 23.5$	

according to specifications. The characteristic impedance $Z_2 = 60\,\Omega$ at input and output ports was selected, so the TL width of W_1 and W_4 are the same. The overall circuit size of the proposed BPF is 34 mm × 20 mm.

In the measurement, the TRL calibration technique was used to offset the lengths of the subminiature version A (SMA) connectors at the reference impedance line of two ports as can be seen in Fig. 9. Then, the unsymmetrical two-port *S*-parameters can be measured and extracted as an S2P file from network analyser. By renormalising, the measured data with respect to the port impedances, i.e. 20 and 50 Ω, the *S*-parameter with port impedances of 20 and 50 Ω can be calculated using ADS.

The photograph of the fabricated circuit, simulated, measured *S*-parameters, and measured group delay of the passband responses is shown in Fig. 10. The measured results agree well with the simulated results. The first spurious frequency occurs at $2.5f_0$. The measured insertion loss is 0.63 dB at the lower band edge of 2.54 GHz, 0.55 dB at f_0 of 2.6 GHz, and 0.65 dB at the upper band edge of 2.66 GHz. The input and output return losses within the whole passband (FBW = 4.6%) are better than 20 dB. Moreover, the lower- and upper-side stopband rejections of 20 dB are obtained from DC to 2.35 and 3.1 to 5.74 GHz, respectively. The measured group delay of the passband is lower than 2.2 ns.

4.2 Antiparallel coupled line two-stage SIR BPF

The second impedance matching BPF was designed with the same specification as that of the first BPF; however, the intermediate coupled lines were designed using an antiparallel coupled line. The overall circuit size of the proposed filter is 47 mm × 13 mm. The photograph of the fabricated circuit, simulated, measured *S*-parameters, and measured group delay of the passband is shown in Fig. 11. The rejection levels at the first spurious frequency of 6.23 GHz in the first BPF are better than 38 dB by the transmission zero. The measured insertion loss is 0.95 dB at the lower band edge of 2.54 GHz, 0.85 dB at f_0 of 2.6 GHz, and 0.97 dB at the upper band edge of 2.65 GHz. Also, the measured input and output return losses within the whole passband (FBW = 4.2%) are better than 19 dB. Moreover, the lower- and upper-side stopband rejections of 25 dB are obtained from DC to 2.23 GHz and 3 to 8.95 GHz, respectively. The first spurious frequency occurs at 9.65 GHz ($3.71f_0$), which is located much higher than the first BPF.

Moreover, the stopband attenuation near to the passband is improved compared to the first impedance matching SIR BPF. The measured group delay of the passband is lower than 2.8 ns.

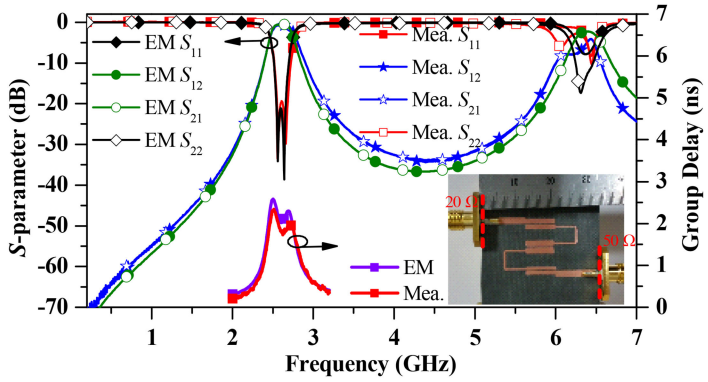

Fig. 10 *Simulated and measured results of two-stage impedance matching SIR BPF using Chebyshev response*

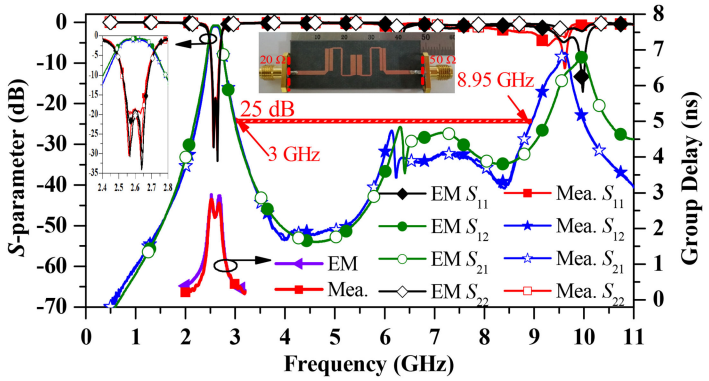

Fig. 11 *Simulation and measured results of two-stage impedance matching SIR BPF with Chebyshev response using the antiparallel coupled line*

Table 5 Performance comparison of the proposed filter with other works

Ref.	f_0, GHz	Termination impedance	n	Spurious	Image impedance	Design equations	PCB/response
[3]	1.2	Z_0	i	A	NA	C	M/BPF
[4]	NA	Z_0	i	A	arbitrary	C	M/BPF
[5]	1.85	Z_0	i	A	arbitrary	C	M/BPF
[7]	2.4	Z_0	even	A	Z_0	C	M/BPF
[10]	3	arbitrary	2	A	NA	C	cavity/BPF
[13]	f_0	arbitrary	even	A	NA	C	NA/LPF
[17]	3	arbitrary	i	A	NA	D	M/BPF
[18]	2.6	arbitrary	i	A	arbitrary	C	M/BPF
[19]	2.6	arbitrary	1	A	arbitrary	C	M/BPF
[22]	2.6	arbitrary	2	A	arbitrary	C	M/BPF
[23]	1	arbitrary	2	A	NA	C	M/BPF
[25]	1	Z_0	i	B	Z_0	C	M/BPF
[26]	2	Z_0	i	A	arbitrary	C	M/BPF
this work	2.6	arbitrary	i	B	arbitrary	C	M/BPF

i = 2 to n, A = uncontrollable, B = controllable, C = analytical, D = optimisation, M = microstrip line

4.3 Three-stage SIR BPF

The third impedance matching BPF was designed for the Chebyshev response with ripple = 0.043 dB, $R_S = 50\ \Omega$, $R_L = 100\ \Omega$, $Z_2 = 90\ \Omega$, $K = 1.5$, $n = 3$, and FBW = 5%. The calculate circuit parameters are shown in Table 5. The overall circuit size of the proposed filter is 30 mm × 57 mm. By choosing $Z_2 = 90\ \Omega$, the physical widths of TLs are calculated to be $W_1 = W_5 = 0.9$ mm. Thus, the filter can be matched to the specific termination impedances at the reference plan although $Z_2 \neq Z_0$. Fig. 12 shows a photograph of the fabricated filter, simulated, measured S-parameters, and measured group delay of the passband. Because $K = 1.5$, the first spurious frequency occurs at $1.8f_0$. The measured insertion loss is 1.75 dB at the lower band edge of 2.54 GHz, 1.6 dB at f_0 of 2.6 GHz, and 1.76 dB at the upper band edge of 2.64 GHz. Also, the input and output return losses are better than 18 dB from 2.54 to 2.64 GHz. The measured group delay of the passband is lower than 7.4 ns. From this measurement results, it must be noted that the spurious can be moved close to the passband with the unequal termination impedance.

Table 5 shows a comparison of the performance of the proposed impedance matching SIR BPFs with the previous works. The proposed work has the advantages of arbitrary termination impedance, controllable spurious frequency, arbitrary image impedance, and n stage resonators when compared with others.

5 Conclusion

An impedance matching BPF with an arbitrary image impedance of parallel/antiparallel coupled line SIR was proposed and studied in this paper. The parallel/antiparallel coupled line SIR BPF can be designed with arbitrary termination and arbitrary image impedance by adding TLs at the input and output ports. Moreover, the general design equations based on multi-stages half wavelength parallel/

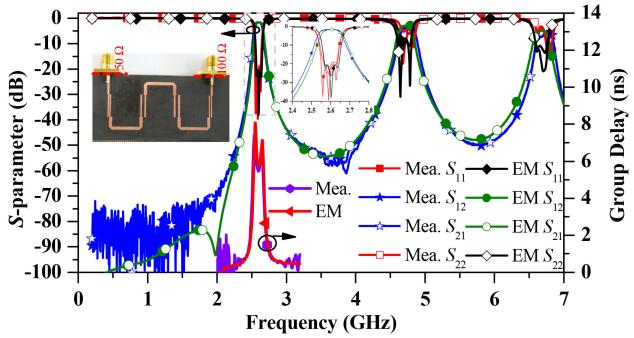

Fig. 12 *Simulated and measured results of three-stage impedance matching SIR BPF using Chebyshev response*

antiparallel coupled line SIR BPFs theory have been derived for the proposed filters. The wide stopband, high selectivity, and high stopband attenuation characteristics are mainly attributed to the antiparallel coupled line. The first spurious frequency of the conventional SIR BPF can be suppressed significantly by a transmission zero for all K. To show the validity of the proposed design formulas, three types of impedance matching SIR BPFs with Chebyshev response were fabricated and measured. The simulated and measured results agree well with the analysis. The proposed method will be advantageous in many applications such as power dividers, impedance matching networks, and power amplifier design. Furthermore, steeper attenuation and wider stopband BPFs with arbitrary termination and arbitrary image impedances based the proposed method will be conducted in the future.

5 Acknowledgments

This research was supported by the Basic Science Research Program through the NRF of Korea, funded by Ministry of Education, Science and Technology (2016R1D1A1B03931400) and partially supported by the Korean Research Fellowship Program through the National Research Foundation (NRF) of Korea, funded by the Ministry of Science and ICT (2016H1D3A1938065).

6 References

[1] Razavi, B.: '*RF microelectronics*' (Prentice-Hall PTR, NJ, Upper Saddle River, USA, 1998), pp. 118–129

[2] Chen, J., Ma, Y., Cai, J., *et al.*: 'Novel frequency-agile bandpass filter with wide tuning range and spurious suppression', *IEEE Trans. Ind. Electron.*, 2015, **62**, (10), pp. 6428–6435

[3] Cohn, S. B.: 'Parallel-coupled transmission-line resonator filters', *IEEE Trans. Microw. Theor. Technol.*, 1958, **6**, (4), pp. 223–231

[4] Swanson, D., Macchiarella, G.: 'Microwave filter design by synthesis and optimization', *IEEE Microw. Mag.*, 2007, **8**, (2), pp. 55–69

[5] Ahn, D., Kim, C., Chung, M., *et al.*: 'The design of parallel coupled line filter with arbitrary image impedance'. IEEE Int. Microwave Symp. Digest, Baltimore, Maryland, USA, 1998, pp. 909–912

[6] Akra, M., Pistono, E., Ferrari, P., *et al.*: 'A novel accurate method for synthesizing parallel coupled line bandpass filter'. 13th Mediterranean Microwave Symp., Saida, Lebanon, 2013, pp. 1–4

[7] Zhang, S., Zhu, L.: 'Synthesis method for even-order symmetrical Chebyshev bandpass filters with alternative J/K inverters and $\lambda/4$ resonators', *IEEE Trans. Microw. Theor. Technol.*, 2013, **61**, (2), pp. 808–816

[8] Lee, H., Tsai, C.: 'Improved coupled-microstrip filter design using effective even-mode and odd-mode characteristic impedance', *IEEE Trans. Microw. Theor. Technol.*, 2005, **53**, (9), pp. 2812–2818

[9] Chen, K., Liu, X., Chappell, W., *et al.*: 'Co-design of power amplifier and narrowband filter using high-Q evanescent-mode cavity resonator as the output matching network'. IEEE Int. Microwave Symp. Digest, Baltimore, Maryland, USA, 2011, pp. 1–4

[10] Chen, K., Lee, J., Chappell, W., *et al.*: 'Co-design of highly efficient power amplifier and high-Q output bandpass filter', *IEEE Trans. Microw. Theor. Technol.*, 2013, **61**, (11), pp. 3940–3950

[11] Chen, K., Lee, T., Peroulis, D.: 'Co-design of multi-band high-efficient power amplifier and three-pole high-Q tunable filter', *IEEE Microw. Wirel. Compon. Lett.*, 2013, **23**, (12), pp. 647–649

[12] Matthaei, G. L.: 'Tables of Chebyshev impedance-transformation networks of low-pass filter form', *Proc. IEEE*, 1964, **52**, (8), pp. 939–963

[13] Cristal, E.: 'Tables of maximally flat impedance-transformation networks of low-pass filter form', *IEEE Trans. Microw. Theor. Technol.*, 1965, **13**, (5), pp. 693–695

[14] Chen, K., Peroulis, D.: 'Design of highly efficient broadband class-E power amplifier using synthesized low-pass matching networks', *IEEE Trans. Microw. Theor. Technol.*, 2011, **59**, (12), pp. 3162–3173

[15] Chen, K., Peroulis, D.: 'Design of broadband highly efficient harmonic-tuned power amplifier using in-band continuous class-F-1/F mode transferring', *IEEE Trans. Microw. Theor. Technol.*, 2012, **60**, (12), pp. 4107–4116

[16] Yang, M., Xia, J., Guo, Y., *et al.*: 'Highly efficient broadband continuous inverse class-F power amplifier design using modified elliptic low-pass filtering matching network', *IEEE Trans. Microw. Theor. Technol.*, 2016, **64**, (5), pp. 1515–1525

[17] Oraizi, H., Moradian, M., Hirasawa, K.: 'Design and optimization of microstrip parallel-coupled line bandpass filters incorporating impedance matching', *IEICE Trans. Commun.*, 2006, **E89-B**, (11), pp. 2982–2988

[18] Kim, P., Chaudhary, G., Jeong, Y.: 'Unequal termination impedance parallel-coupled lines band-pass filter with arbitrary image impedance', *J. Electromagn. Wave Appl.*, 2018, **32**, (8), pp. 984–996

[19] Kim, P., Chaudhary, G., Jeong, Y.: 'Enhancement impedance transforming ratios of coupled line impedance transformer with wide out-of-band suppression characteristics', *Microw. Opt. Technol. Lett.*, 2015, **57**, (7), pp. 1600–1603

[20] Kim, P., Jeong, J., Chaudhary, G., *et al.*: 'A design of unequal termination impedance power divider with filtering and out-of-band suppression characteristics'. Proc. of the 45th European Microw. Conf., Paris, France, 2015, pp. 123–126

[21] Jeong, J., Kim, P., Jeong, Y.: 'High efficiency power amplifier with frequency band selective matching networks', *Microw. Opt. Technol. Lett.*, 2015, **57**, (9), pp. 2031–2034

[22] Kim, P., Chaudhary, G., Jeong, Y.: 'Ultra-high transforming ratio coupled line impedance transformer with bandpass response', *IEEE Microw. Wirel. Compon. Lett.*, 2015, **25**, (7), pp. 445–447

[23] Wu, Q., Zhu, L.: 'Synthesis design of a wideband impedance transformer consisting of two-section coupled lines', *IET Microw. Antennas Propag.*, 2017, **11**, (1), pp. 144–150

[24] Sagawa, M., Makimoto, M., Yamashita, S.: 'Geometrical structures and fundamental characteristics of microwave stepped-impedance resonators', *IEEE Trans. Microw. Theor. Technol.*, 1997, **45**, (7), pp. 1078–1085

[25] Makimoto, M., Yamashita, S.: 'Bandpass filter using parallel coupled stripline stepped impedance resonators', *IEEE Trans. Microw. Theor. Technol.*, 1980, **28**, (12), pp. 1413–1417

[26] Worapishet, A., Srisathit, K., Surakampontorn, W.: 'Stepped-impedance coupled resonators for implementation of parallel coupled microstrip filter with spurious band suppression', *IEEE Trans. Microw. Theor. Technol.*, 2012, **60**, (6), pp. 1540–1548

[27] Matthaei, G. L., Young, L., Jones, E. M. T.: '*Microwave filter, impedance-matching networks and coupling structures*' (McGraw-Hill, New York, NY, USA, 1964)

[28] Makimoto, M., Yamashita, S.: '*Microwave resonators and filters for wireless communication*' (Springer-Verlag, Berlin, Heidelberg, 2001)

[29] Pozar, D. M.: '*Microwave engineering*' (John Wiley & Sons, 2012, 4th edn.)

[30] Hong, J. S.: '*Microstrip filter for RF/microwave application*' (John Wiley & Sons, 2011, 2nd edn.)

[31] Zhang, S., Zhu, L., Weerasekera, R.: 'Synthesis of inline mixed coupled quasi-elliptic bandpass filters based on $\lambda/4$ resonators', *IEEE Trans. Microw. Theor. Technol.*, 2015, **63**, (10), pp. 3487–3493

[32] Zhang, S., Zhu, L., Li, R.: 'Compact quadruplet bandpass filter based on alternative J/K inverters and $\lambda/4$ resonators', *IEEE Microw. Wireless Compon. Lett.*, 2012, **22**, (5), pp. 224–226.